Optimization of concentric-tube robot design for deep anterior brain tumor surgery

Mohamed Nassim Boushaki, Chao Liu, Benoît Herman, Vincent Trévillot, Mohamed Akkari, Philippe Poignet

Optimization of Concentric-Tube Robot Design for Deep Anterior Brain Tumor Surgery

Mohamed Boushaki[1], Chao Liu[1], Benoît Herman[2], Vincent Trevillot[3], Mohamed Akkari[3] and Philippe Poignet[1]

***Abstract*— Most of existing works on the tubes design optimization of concentric-tube robot (CTR) do not include the elastic stability in the optimization criteria. The only work which formulates the elastic stability in the objective function is based on scalarization method which is used in existing multi-objective design optimization. The objective function is formed by a set of weighted objective functions. The selection of the weights is crucial as the optimization results are greatly affected by them and could be misleading if these weights are improperly chosen. As an alternative optimization technique, we use Pareto grid-searching method to avoid this problem and allow a straightforward interpretation of the results following the selection criteria for the parameters to be optimized. This paper shows a three-tube CTR design based on Pareto grid-searching method in order to optimize the reachability and elastic stability of the CTR within a specific curvature range dedicated to the deep anterior brain tumor removal surgery.**

I. INTRODUCTION

Typical surgical robots for Minimally Invasive Surgery (MIS) use rigid and straight instruments with an articulated tip. Small sized flexible robots are more suitable for MIS as they can reach surgical sites of high access difficulty [1].

Concentric Tube Robots (CTR) belong to this category of flexible robots with the advantages of good steerability, controllability of the shape and small size. During last decade, CTR has drawn considerable attention [2] [3]. CTR is a kind of flexible robot whose concept is to insert concentrically pre-shaped flexible Nitinol tubes such that each of them is endowed with an axial rotation and linear translation. Previous works show the potential of using this technology in many medical applications, such as neurosurgery [4], intracardiac surgery [5], endonasal skull base surgery [6] and lung biopsy[7].

It is obvious that the design of the CTR tubes differs from one medical application to another. The tubes dimensions depend mainly on the specific task and the involved anatomical structure. To meet various performances indices, the robot tubes design should be optimized accordingly. The evolution of CTR tube design optimization can be traced from three aspects. Firstly, the design optimization follows the advances in kinematics modeling. In the early works on tubes design optimization, only basic kinematic model was used [5] [6]. Later on, more accurate kinematics model has been involved [9]. With more accurate kinematics, better robot design optimization could be obtained since the kinematic model is involved in the optimization calculation. Secondly, the design optimization evolution could also be analyzed from the view of clinical applications tackled seeing that many specific design optimization algorithms have been proposed for different clinical procedures [4] [5] [6] [7]. And another axis of this evolution is the transition from considering a discrete set of point in the objective function to a volume-based objective functions [9].

Elastic instability is a big challenge for CTR, which may occur when the difference of tube angles in the base of the robot is at the neighborhood of π. The rotation angle difference of the tubes at the distal part has no unique solution in the case of elastic instability, which generates a jump at this distal proximity (snapping)[16]. The elastic stability decreases once the tubes curvatures and/or lengths increase, and when it drops below the stability limit the snapping phenomenon appears. Elastic instability could lead to serious safety problem during the robotized intervention if it has not been considered in the robot design or in the path planning.

The problem of elastic instability was not taken into account in CTR tube design optimization in literature until the work of [17], but it is limited to a particular case of two planar tubes with variable pre-curvature of the tubes. Bergeles et al. in [11] have shown a way to analyze the stability when the number of tubes exceed two, but it is not applicable for arbitrary number of tubes. In [11], the formulation of the optimization problem is based on scalarization method, and the objective function is a concatenation of weighted sub-objective functions which makes the results highly dependent on the a-priori weights. The selection of the weights is a not-trivial and crucial task.

The targeted surgical application of our work presented in this paper is deep frontal lobe brain tumors where elastic instability is of high risk to the operation safety. Therefore, in this work the elastic stability is explicitly considered as an optimization criterion. Instead of scalarization method, a Pareto grid-searching method has been used which incorporates all performance criteria within the optimization process and address them simultaneously to find a set of non-dominated designs in the objective space [15] and therefore

This work was partially supported by the French Investissements d'Avenir program (Labex CAMI) under reference ANR-11-LABX-0004.

[1] M. N. Boushaki, C. Liu and P. Poignet are with LIRMM, UMR5506, University of Montpellier, France boushaki;liu;poignet@lirmm.fr

[2] B. Herman is with University Catholic of Louvain, Louvain-la-Neuve, Belgium benoit.herman@uclouvain.be

[3]V. Trevillot and M. Akkari are with the University Hospital of Montpellier, Montpellier, France v-trevillot@chu-montpellier.fr, mohamed.akkari.orl@gmail.com

avoid the weight choice problem. The objective is to find the tube curvatures which suit best the specifications of the addressed surgical application. Other parameters such as robot structure, lengths of the tubes, and variation intervals of the curvatures to be optimized are pre-selected based on CT scan images in order to respect the anatomical constraints during the insertion and to be as close as possible to the optimal parameters with the help of surgeons.

Another contribution of this work is to use the forward kinematic model in the objective function instead of the inverse kinematics which has been used in [5] [11] to avoid the anatomical obstacles. The inverse kinematic model is complex and time consuming to calculate, and it requires a numerical optimization to be solved. The forward kinematic model used in this work is the torsionally compliant model developed in [16]. Two mappings are required to obtain the pose G of the robot tip. The first one is to calculate the curvatures and the rotation angles of the tubes along the whole robot shaft in terms of the joint variables (base rotations and translations). This mapping is modeled by a function f_1 which is a nonlinear differential equation system with problem of boundary conditions. The second mapping f_2 is to integrate geometrically the obtained curvature $u(s)$ in order to define the robot shaft including the tip pose. Based on the optimal parameters, the tubes are to be fabricated to integrate to our CTR system.

II. Multicriteria optimization using Pareto methods

The mathematical formulation of a multi-objective optimization problem can be described as follows:

$$\begin{aligned} &\min_x \{\varphi_1(x),\, \varphi_2(x),\, ...\varphi_n(x)\} \\ &subject\,to\, x \in \varpi \end{aligned} \tag{1}$$

where $n > 1$, x is the decision variables vector, φ_i are the objective functions constituting the objective space, and ϖ is the set of constraints [19]. A decision vector $x^* \in \varpi$ is the Pareto optimal vector for a multi-objective problem if all other vectors $x \in \varpi$ cause higher values for at least one objective function φ_i or have the same values for all φ_i. The collection of all the efficient solutions is called Pareto curve. The trade-off between objective functions is concluded from this Pareto curve.

A. Scalarization technique

Among all methods to solve Pareto optimal solutions for multi-criteria optimization, the scalarization method is the most commonly used one. In scalarisation method, the objective functions to be minimized are transformed to a single-objective scalar function by affecting weighting and summing them [18]. The new objective function is defined as:

$$\begin{aligned} &\min_x \sum_{i=1}^{n} \omega_i \cdot \varphi_i(x), \qquad \sum_{i=1}^{n} \omega_i = 1, \qquad (\omega_i > 0) \\ &subject\,to\, x \in \varpi \end{aligned} \tag{2}$$

The minimum of this new optimization objective belongs to the Pareto curve. This method is easy to understand and implement. However, as the weights are pre-selected, they may not correspond to the relative importance of the objective functions. It is also difficult to change the weights or to find an heuristic iterative variation low making them change in order to reach a part of the Pareto curve. Moreover, selecting different weights vectors to perform several optimizations (in order to reach more parts of the Pareto curve) causes a large computational burden. Two other limitations of this scalarization technique are: a uniform spread of the weights does not produce a uniform propagation of the Pareto curve points i.e. some points of the former have not been considered; non-convex Pareto set parts are not reachable with the minimization of convex combinations of the objective functions.

B. Grid-searching technique

This technique allows to avoid the drawbacks of scalarization previously introduced due to the preselection of the weights. Three steps are to be followed in order to define the best trade-off between objective functions:

- First, the Pareto set is generated by taking a sampling grid of the decision space x and then to calculate their corresponding objective functions. The obtained points are plotted in the objective space as illustrated in Fig.1, where the Pareto curve can be approximated by a polynomial.
- The next issue after tracing the Pareto set is to find the

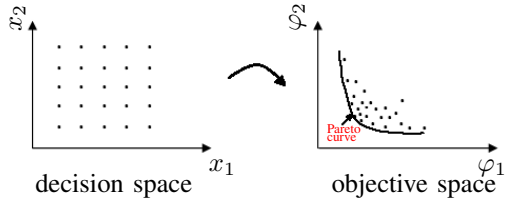

Fig. 1: Mapping from decision space to objective space.

suitable solution on it. Many approaches have been proposed in literature to solve this problem. The approach used in this work is the No-preference approach assuming "equal importance" of each criterion where the mostly used way to find the best solution is to calculate the L_2 norm for all the points as follows:

$$D_{L_2}(x) = \sqrt{\sum_{i=1}^{n} (\varphi_i(x) - \varphi_i^{min})^2}, \tag{3}$$

where φ_i^{min} is the minimum of φ_i, and then to select the point corresponding to the minimum of this distance [18]. In case of maximization of the objective functions, the maximum of the L_2 norm is used. Note that if the equal importance of the objective functions is not considered, then one of the plot axes should be scaled before calculating the L_2 norm, and this scale corresponds to the weights.

- The last step is to map from the Pareto set back to the decision space. There are many methods in literature which

ensure this mapping such as intersection of constant objective contours, etc. However, in this work we select the decision variables that correspond to the optimal objective solution obtained in the previous step.

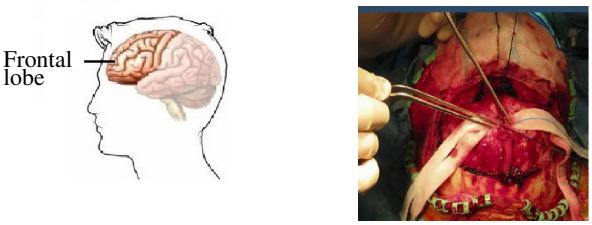

(a) frontal lobe (b) intervention

Fig. 2: Transcranial intervention for frontal lobe tumor resection

III. Targeted surgical application

In this work, the specific surgical application is considered; removal of deep frontal lobe brain tumors cf. Fig.2.a. It is noted that in year 2012, 70 % of the over 250 000 patients with brain tumor died in the world [10]. Usually for anterior skull base surgery, the procedure is transcranial, the access is created by severing a portion of the cranium. The surgeon needs to gently lift up the brain to access to the deep tumor located under the brain in order to accomplish the resection procedure cf. Fig.2.b. Following this procedure, the brain will swell up after the operation, which creates a brain pressure and causes a large trauma for the patient. To alleviate this problem, an endonasal approach is proposed by using CTR which is flexible and adaptable with the anatomical complexity. Note that, similar as the case in [6] which addresses pituitary gland tumor removal, this operation requires bone drilling in order to access to the surgical site and reach the tumor. But the insertion path in our case from the nostril to the anterior wall of the frontal sinus (location of the drilling point) is surrounded with structures of high sensitivity cf. Fig.3.a and Fig.3.b. Another challenge of the targeted surgical application is the no-coaxiality of the insertion path with the tumor location increases the complexity of accessibility to the surgical site.

IV. Workspace characterization and anatomy

Given the sagittal and coronal planes CT scan images of a real patient case study, a base frame F_b is attached to the patient head with its origin O close to the nose and centered at the median between the two nostrils as shown in Fig.3. The Z axis is oriented from the nose to the head back, the Y axis is oriented from the nose to the head top. The insertion point of the robot is at P point in Fig.3.a and Fig.3.b, with P defined as the origin of the robot frame F_r. The orientation of F_r is decided by two rotations: ϕ which orients the robot from the nostril to the frontal sinus in the Y-Z plan of the frame F_b and allows to avoid the nasal turbinates; and The ψ which orients the robot to the left or to the right of the cerebral falx depending on the tumor location. Based on CT scan images and with more clarification and orientation of the surgeon, the space of the passage used to introduce the CTR from the nostril to the frontal sinus is identified roughly as a straight tunnel with variable diameter (from $\approx 10mm$ for smaller ellipse diameter to $\approx 30mm$ for bigger ellipse diameter) and a length of $\approx 72mm$ for the patient sample studied. These allowed workspace borders are illustrated by six green ellipses in Fig.3. These anatomical constraints (orbits, optic canal, nerves...) should be considered in an eligibility criterion. In order to reduce the friction during the robot insertion, a large passive tube is pre-inserted before introducing the robot. This facilitates the insertion of the robot in the first part of its path which is characterized by high friction according to the surgeons. Once the navigation path is traversed, the distal section of the robot accesses to the anterior skull base to manipulate at the tumor location.

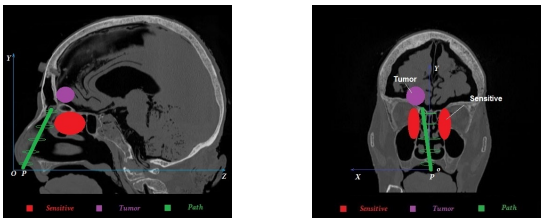

(a) sagittal plane (b) coronal plane

Fig. 3: Work-space characterization

A scenario of a sphere tumor defined by its center position coordinates c and its radius $a = 10\ mm$ is shown by purple color in Fig.3. The frequent scenario in reality is that the tumor is located at the left of at the right of the frontal lobe.

V. CTR configuration selection

By considering the aforementioned anatomical description, a robot configuration is proposed in this section following the surgeons advices.

A. Kinematics description

To fulfill accessibility and dexterity requirement, the candidate robot to be optimized is a three-tube CTR. The outermost tube $T1$ is straight and the other two tubes $T2$ and $T3$ have two parts (straight and curved) as shown in Fig.4. The tubes deployment (see Fig.4) decides the number of tubes existing in one section, the number of sections, their order, lengths and curvatures (constant or variable curvature). In terms of reachability, the proposed configuration allows to benefit from both advantages of constant curvature and variable curvature of the robot distal section. The distal section can be composed by two pre-curved tubes which is a variable curvature section (S_{B4}) or by only one pre-curved tube which means a constant curvature section (S_{C5}) as seen in Fig. 4. The translation limits, and the curved and straight tube lengths define this transition constant/variable curvature of the distal section. The distal section manipulates the tool to accomplish the requested task (grasping, aspiration, electrocoagulation etc). For the proposed robot structure, the constant curvature section allows to reach the regions far

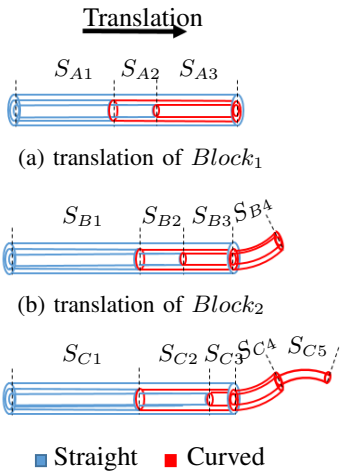

(a) translation of $Block_1$

(b) translation of $Block_2$

(c) translation of $Block_3$

Fig. 4: Robot shaft sections

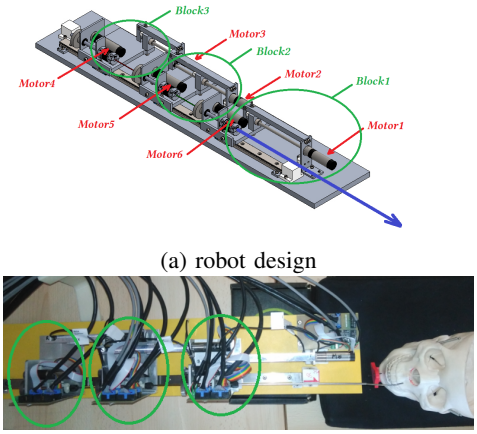

(a) robot design

(b) CTR platform

Fig. 5: Robot

TABLE I: Notations and Dimensions

F_b: base frame, its origin is O, F_r: robot frame, its origin is P
ϕ: X-rotation angle of Rob, ψ: Y-rotation angle of Rob after its X-rotation
c: tumor center coordinates
f_1: solves the nonlinear differential equation system of the forward kinematic model
f_2: numerical integration of the curvatures $u(s)$ to define the robot shape
$G(s)$: homogeneous matrix of the pose of a point s from the robot shaft
k_2,k_3: curvatures of tubes T_2 and T_3 expressed in mm^{-1}
Δq: sampling step of the rotation joints, Δs: sampling length
χ: cartesian tip position in F_b
a: radius of the sphere tumor $= 10\ mm$
l_{s1}: length of the straight part of $T_1 = 70\ mm$, l_{s2}: length of the straight part of $T_2 = 30\ mm$
l_{c2}: length of the straight part of $T_3 = 31\ mm$, l_{s1}: length of the curved part of $T_2 = 41\ mm$
l_{s2}: length of the curved part of $T_3 = 43\ mm$
Δk: curvature sampling step in the refining $= 10mm^{-1}$
$k_2 = 55 : \Delta k : 70mm^{-1}$,$k_3 = 35 : \Delta k : 50mm^{-1}$

from the centerline of the robot shaft and the regions close to it could be reached by a variable curvature distal section.

B. Actuation description

Concerning the actuation unit, it is composed of three blocks with one for each tube. Note that for the proposed actuation unit and for each tube, the rotation and translation are decoupled. Thanks to this decoupling, each rotation is controlled by one dedicated motor, which improves the control performance, facilitates the calibration procedure and reduces the modeling complexity. The tubes translations are produced by the blocks translations, which are ensured by the rotations of a nut-screw systems and guidance rails (see Fig. 5). Once a block translates, it pulls the blocks behind it. This mechanism allows to reduce the tubes lengths and hence the tubes torsions. The $Block1$ (front block) is dedicated to the outer-most tube T_1, and the $Block3$ (arrear block) is dedicated to the inner-most one T_3. The insertion of the robot from the nostril till the frontal sinus is ensured by the translation of the $Block1$ which pulls the two other blocks, producing a translation of the three tubes simultaneously. The distal proximities of the tubes are at the same limit. The shape of the robot shaft is held during this insertion. After this navigation insertion, the tube $T1$ is held, then if only $Block2$ is translated, the distal section of the robot is a variable curvature section (see Fig.4b), otherwise a part of the inner-most tube $T3$ extends out of tube $T2$ and forms a distal constant curvature section. Once the distal extremity of the robot accesses to the anterior cranial fossa through the posterior table of the frontal sinus, tube $T2$ and/or $T3$ are/is actuated in rotation and/or translation to accomplish the manipulation task.

VI. Formulation of Grid-Searching Optimization Algorithm for CTR

A. Decision space

For our specific surgical application, the manipulation part of the robot extends from the drilling point to the posterior part of the tumor. For a such distance, the lengths of the curved parts of the two inner tubes do not have significant effect on the optimization results. Moreover, reducing the number of decision parameters allows to decrease the computation time significantly. The lengths of tubes are then pre-selected suitable for the task respecting the workspace and anatomical constraints. The curvatures k_2 and k_3 of the tubes $T2$ and $T3$ respectively are considered as the decision variables. The localization of their ranges is firstly estimated from the geometry of the anatomical constraints, then obtained by executing the Algorithm.1 as introduce later.

B. Objective space

The objective space is defined by two criteria (objective functions):

• Reachability criterion: In order to evaluate the reachability of the surgical workspace (tumor), this workspace is sampled homogeneously to a set of points $W(i)$. Once the euclidean distance between the workspace center and the tip position is less or equal than the work-space radius a, we check which point from $W(i)$ is closer to this tip position, and we increase the score of reachability of this point $W(i)$. For a given configuration (k_2, k_3), a point from $W(i)$ can be reached more than once. Consider m is the number of

the point reached from $W(i)$, and n is the number of the work-space samples points, the reachability is evaluated as:

$$C_{reach}(k_2, k_3) = \frac{m}{n} \times 100 \tag{4}$$

• Stability criterion: For the elastic stability analysis, previous works rely on the evolution of the difference of distal tubes angles in terms of the base difference tubes angles [16]. There is no systematic and general approach so far which allows to evaluate the elastic stability once the tube number exceed three. The case of three tubes has been treated by Bergeles et al in [11].

In this work, a new way of stability evaluation is proposed. It relies on numerical evaluation of the tip trajectory smoothness. In case of elastic instability, jumps appear in the robot tip trajectory even if the tubes rotations variations are continuous and smooth. The elastic stability could be quantified by evaluating the euclidean distance $\sqrt{\chi^2(1) + \chi^2(2)}$ covered by the robot tip, since the robot shaft rotation is around the Z axis. In order to find out the jumps (case of instability) on the distal angle difference in ascending and descending, the $bvpinit$ Matlab function is used to select the symmetric solution which shows a distal angle jump leading to a tip position jump. The new proposed approach is to quantify these jumps or discontinuities of the robot tip trajectory. Firstly, the numerical derivative of the euclidean distance in term of the joint variation (rotation sampling step) is calculated for each configuration (k_2, k_3), then the standard deviations of these derivatives are calculated. The stability of a given configuration (k_2, k_3) is inversely proportional to the derivative standard deviation.

$$C_{stab}(k_2, k_3) = normalization(1/std(\frac{\Delta\sqrt{\chi^2(1) + \chi^2(2)}}{\triangle q})) \tag{5}$$

C. Constraints

The first constraint is to consider only the decision variables satisfying $(k_2 < k_3)$ during the grid sampling. This heuristic condition is recommended in [16] because the proximal sections are constrained by the navigation path and then should be of small curvature. Moreover, the distal sections which are composed of inners tubes dedicated to manipulate the tip should be with high curvatures. The second constraint is defined by an eligibility condition under the notation C_{eli}. The confliction of the robot shaft with the anatomical structure is checked using the ellipses borders. Once the Y coordinate of the robot $\chi(2)$ is equal to the Y coordinate as an ellipse, this shaft robot point is checked to see if it is inside the ellipse or not by using the two radii of the ellipse to calculate the distance from the borders. The robot shaft is considered satisfying the eligibility condition if and only if each point of the robot which has the same Y coordinate of an ellipse is inside its corresponding ellipse. This condition is first to be checked, i.e the configurations outside of the borders are rejected and will not be evaluated in the reachability and stability criteria.

D. Grid-searching algorithm execution

After the first execution of the Algorithm.1 with large sampling interval $(15mm^{-1})$ which allows to locate the variation ranges of the decision variables (k_2, k_3) ; where the optimal decision variables intervals corresponding to the highest reachability and stability may lie in. A second execution is conducted with smaller sampling interval $(5mm^{-1})$ to ensure a finer mapping from the decision variables(k_2, k_3) to the objective space (C_{stab}, C_{reach}). For each configuration, (k_2,k_3) of the grid satisfying $(k_2 < k_3)$, the eligibility condition C_{eli} is checked. If it is respected, then two selection criteria are evaluated, i.e. the *stability criterion* C_{stab} and the *reachability criterion* C_{reach} as defined in last subsection. In the end, the criteria C_{stab} and C_{reach} are evaluated along all the configurations satisfying the eligibility condition. The next step is to calculate the L_2 norm of all obtained solutions in the objective space. As the objective of this optimization problem is to maximize both objective functions, the solution with highest L_2 norm is chosen and their corresponding (k_2, k_3) are defined as the optimal decision variables.

Algorithm 1

Initialization:
$Reachable(W(i)) = 0$ with $i = 0 : n$
for $k_2 = k_{2init} : k_{2fin}$, $k_3 = k_{3init} : k_{3fin}$ **do**
  $config++$
  for $d_2 = 0 : d_{2fin}$, $d_3 = 0 : d_{3fin}$, $\theta_2, \theta_3 = 0 : 2\pi$ **do**
    $u(s) = f_1(k_2, k_3, d_2, d_3, \theta_2, \theta_3)$
    $G(s) = f_2(u(s))$
    if $\chi(2) = Y_{borders}$ **then**
      if the shaft is inside the ellipses borders **then**
        Test Reachability:
        if $\| \chi - c \| \leq a$ **then**
          $ind = index(min(\chi - W(i))$
          $Reachable(config, ind)++$
          $save(\chi)$ to be used in C_{stab} evaluation
          $save(Reachable(config))$ to be used in C_{reach} evaluation
        end if
      end if
    end if
  end for
end for
Calculate $C_{stab}(config)$ for all configurations
Calculate $C_{reach}(config)$ for all configurations

VII. Results and discussions

The grid-searching optimization method as explained in last section was executed twice: the first time with larger parameters interval, (k_2, k_3) and curvatures sampling resolution, then the second time to refine the optimization procedure with smaller parameters interval and curvature sampling. In order to accelerate the computation, the algorithm has been run on a server with the characteristics: *Intel(R) Xeon(R), CPU E5-2695-v3 2.30GHz, (27 cores / 396 Go ram).*

As the stability evaluation approach is new, the results obtained through the second execution are interpolated and shown in Fig.6. It can be seen from this illustration that the

stability criterion index increases along both X and Y axis, i.e. the curvatures (k_2, k_3) are decreasing (curvature radii are increasing) which is consistent with the evolution stability in terms of curvatures presented in [16].

Theoretically, the reachability improves by increasing the curvatures. However, in our study this rule can not be well satisfied as the anatomical obstacles are considered along the whole robot shaft, i.e. many points from the workspace are eliminated by the eligibility condition (the reason why the number of points in Fig.7 is restricted (16 points) is because of the fact that non-suitable solutions have already been eliminated in the first execution of the algorithm).

From the mapping to the objective space shown in Fig.7, the solution with highest L_2 norm with respect to the P_{min} of coordinates $(min(C_{reach}), min(C_{stab})) = (0,46,\ 0,48)$ is selected $(D_{L_2} = 0.5631)$. The point P_{opt} surrounded by a black circle is the one with highest L_2 norm, and all the other points corresponding to solutions with different decision variables $(k_2,\ k_3)$ are included in the big blue circle with a radius equal to the D_{L_2}. The coordinates of this solution point corresponding to the reachability and stability respectively are $(0.72,\ 0.99)$. The decision variables corresponded to this solution point P_{opt} are $k_2 = \frac{1}{70}mm^{-1}$, $k_3 = \frac{1}{50}mm^{-1}$.

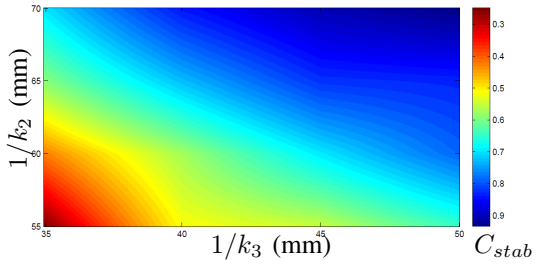

Fig. 6: Stability evaluation

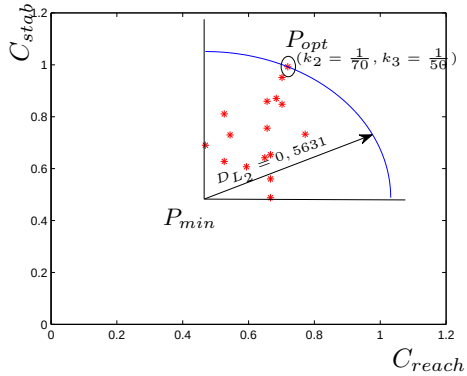

Fig. 7: Stability/Reachability selection

VIII. Conclusion

In this work, a new optimization method for CTR design is presented using grid-searching Pareto which avoids the weight pre-selection problem of scalarization optimization methods. A new approach for elastic stability evaluation was proposed. Based on the specific task requirements and the proposed optimization method, optimal tube parameters can be decided following the proposed optimization approach. The obtained optimized tubes parameters will be used to curve the tubes to be integrated to our CTR platform, and the addressed deep tumor removal surgical procedure will be tested through *ex vivo* lab test and *in vivo* cadaver test.

References

[1] J. Burgner-Kahrs and D. C. Rucker and H. Choset, Continuum Robots for Medical Applications: A Survey, IEEE Transactions on Robotics, pp. 1261-1280, 2015.

[2] P. Sears, and P. E. Dupont, A Steerable Needle Technology Using Curved Concentric Tubes. IEEE/RSJ International Conference on Intelligent Robots and Systems 2006, pp. 2850 - 2856.

[3] R. J. Webster III, A. M. Okamura, and N. J. Cowan, Toward active cannulas: Miniature snake-like surgical robots. IEEE/RSJ International Conference on Intelligent Robots and Systems 2006, pp. 2857 - 2863.

[4] T. Anor, J. R. Madsen, and P. Dupont, Algorithms for Design of Continuum Robots Using the Concentric Tubes Approach: A Neurosurgical Example. IEEE International Conference on Robotics and Automation 2011, pp. 667-673;

[5] C. Bedell, J.Lock, A. Gosline,and P. E. Dupont Design Optimization of Concentric Tube Robots Based on Task and Anatomical Constraints. IEEE International Conference on Robotics and Automation, 2011, pp.398-403.

[6] J. Burgner, P. J. Swaney, D. C. Rucker,H. B. Gilbert, S. T. Nill, P. T. Russell III, K. D. Weaver, and R. J. Webster III, A Bimanual Teleoperated System for Endonasal Skull Base Surgery. IEEE/RSJ International Conference on Intelligent Robots and Systems, 2011, pp. 2517 - 2523.

[7] L. G. Torres, R. J. Webster III, and R. Alterovitz, Task-oriented Design of Concentric Tube Robots using Mechanics-based Models. IEEE/RSJ International Conference on Intelligent Robots and Systems 2012. pp. 4449 - 4455.

[8] D. Caleb Rucker and R. J. Webster III, Mechanics of Bending, Torsion, and Variable Precurvature in Multi - Tube Active Cannulas, IEEE International Conference on Robotics and Automation,2009, pp. 2533-2537.

[9] J. Burgner, H. B. Gilbert and R. J. Webster III, On the Computational Design of Concentric Tube Robots: Incorporating Volume-Based Objectives, IEEE International Conference on Robotics and Automation,2013, pp. 1185-1190.

[10] http://globocan.iarc.fr

[11] C. Bergeles, A. H. Gosline, N. V. Vasilyev, P. J. Codd, P. J. del Nido, and P. E. Dupont, Concentric Tube Robot Design and Optimization Based on Task and Anatomical Constraints. IEEE Transactions On Robotics, Vol. 31, NO. 1, February 2015, pp.67-84

[12] P. E. Dupont, J. Lock and E. Butler, Torsional Kinematic Model for Concentric Tube Robots. IEEE International Conference on Robotics and Automation, Japan, May 12-17, 2009, pp, 3851-3858.

[13] R. M. Murray, Z. Li, and S. S. Sastry, A Mathematical Introduction to Robotic Manipulation. Boca Raton, FL: CRC, 1994.

[14] R. Xu and R. V. Patel, A Fast Torsionally Compliant Kinematic Model of Concentric-Tube Robots. Annual International Conference of the IEEE EMBS San Diego, California USA, 2012, pp, 904-907.

[15] R. Unal, G. Kiziltas, and V. Patoglu, Multi-criteria Design Optimization of Parallel Robots, IEEE Conference on Robotics, Automation and Mechatronics, 2008, pp.112-118.

[16] P. E. Dupont,J. Lock, B. Itkowitz, and Evan Butler, Design and Control of Concentric-Tube Robots. IEEE Transactions on Robotics, VOL. 26, NO. 2, 2010, pp. 209 - 225.

[17] J. Ha, F. C. Park, and P. E. Dupont, Achieving Elastic Stability of Concentric Tube Robots Through Optimization of Tube Precurvature, IEEE/RSJ International Conference on Intelligent Robots and Systems, IROS 2014.

[18] E. M. Kasprzak and K. E. Lewis, "An approach to facilitate decision tradeoffs in Pareto solution sets," Journal of Engineering Valuation and Cost Analysis, vol. 3, no. 1, pp. 173-187, 2000.

[19] M. Caramia and P. DellOlmo, Multi-objective Management in Freight Logistics, Springer, 2008